Collective Excitations of Superfluid Helium

DCS Team: Craig Brown, Nick Butch, Timothy Prisk, and Wei Zhou

Abstract

In this experiment, we will use inelastic neutron scattering to study the collective excitations of superfluid ^{4}He as a function of temperature and pressure. The scattering angle- and time- resolution of the Disk Chopper Spectrometer will allow us to map the momentum-energy dependence of these excitations.

1 Introduction

Neutron scattering techniques provide experimentalists with direct probes of the atomic-scale structure and dynamics of materials[1]. An important application of inelastic neutron scattering is the study of the collective excitations in condensed matter systems, such as the lattice vibrations and spin waves of crystalline materials. Determining the dispersion relation of these excitations is an important task for an experimentalist, as this information is a clue about the strength of intermolecular interactions as well as the thermodynamic and transport properties of the material. In this experiment, we will explore the excitations of a *quantum fluid*, namely liquid ^{4}He.

Figure 1 illustrates the pressure-temperature phase diagram of ^{4}He. Also shown is a generic phase diagram of an ordinary classical fluid. A striking difference between these two phase diagrams is the fact that ^{4}He remains a liquid down to absolute zero temperature under its own vapor pressure. Solification only occurs if an external pressure (>25 atm) is applied to it. If a substance is comprised of atoms/molecules which obey classical mechanics, then that substance must crystallize or solidify if the temperature is reduced sufficiently low. The gain in potential energy obtained by localizing the atoms at specific sites is large enough to overcome the kinetic energy of thermal motion. Two different properties of helium atoms combine to destabilize the solid phase: the light mass of helium atoms and the weakness of interatomic attraction. Because helium atoms have a small mass, they have a relatively large amount of quantum-mechanical zero-point energy. This energy is comparable to the depth of the attractive potential well, thereby preventing crystallization unless external pressure is applied.

Another striking aspect of the phase diagram shown in Figure 1 is the fact that ^{4}He has two different liquid phases, referred to as He-I and He-II. When liquid helium is cooled below a critical temperature T_λ, it undergoes a second-order phase transition from a *normal fluid* (He-I) to a *superfluid* (He-II). Normal fluids possess a finite viscosity: they resist shearing and their currents steadily dissipate in the absence of driving forces. In addition, a normal fluid has finite thermal conductivity, making diffusion a mechanism by which heat is transported through the fluid. Lastly, there are no fundamental constraints on the amount of rotational flow in normal liquids. The properties of superfluids are radically different in all three respects. Superfluid helium is capable of flowing with exactly zero viscosity, and so under appropriate circumstances it exhibits dissipationless flow! It has infinite thermal conductivity and so, unlike normal fluids, it cannot support static temperature gradients. Instead, temperature and entropy propagate through superfluids in the form of waves known as 'second sound.' Finally, circulation in superfluid helium occurs within quantized vorticies which are analogous to the flux-vortex lines observed in superconductors. The properties of He-II, and their roots in Bose-Einstein condensation, are discussed in the books by Annett[3] and Pitaevskii and Stringari[4].
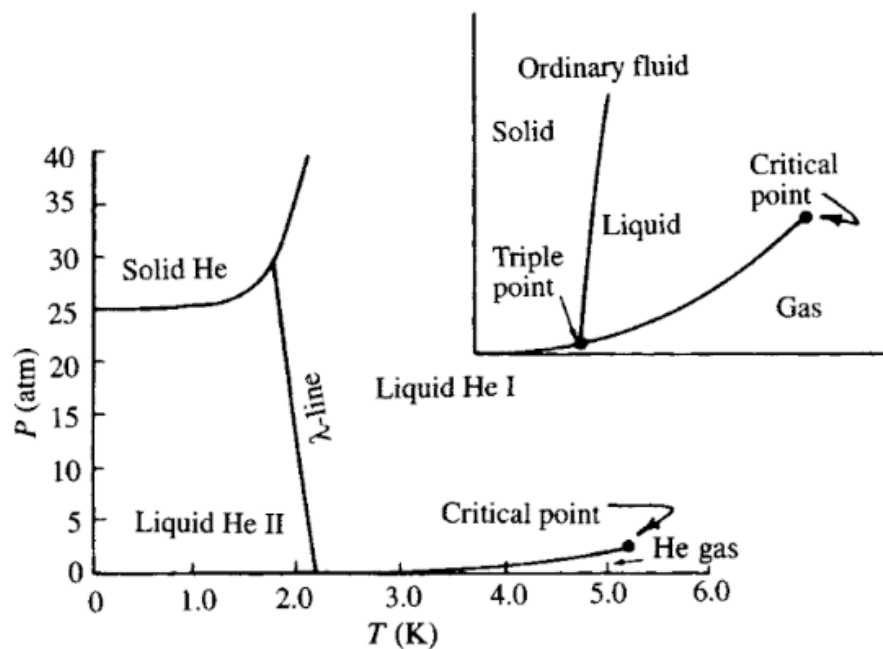
Figure 1: The pressure-temperature phase diagram of ^{4}He compared with an 'ordinary' fluid[2].
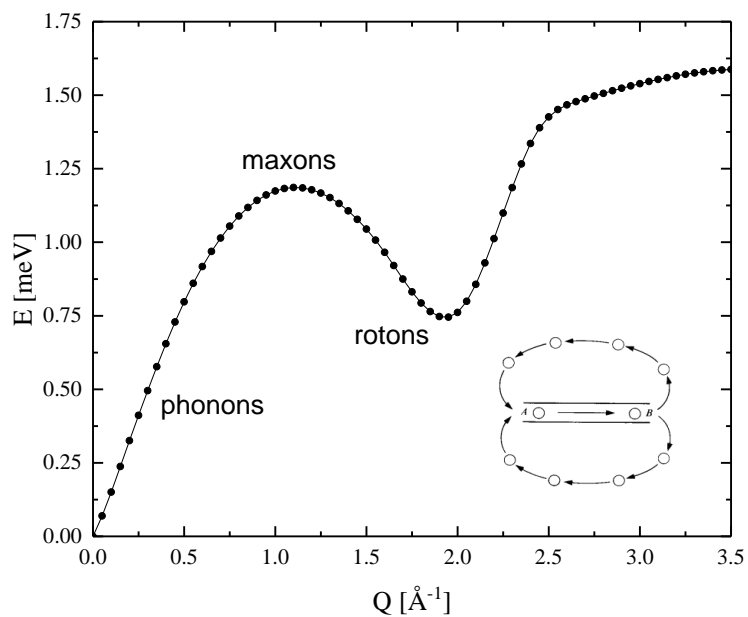

Figure 2: The elementary excitation spectrum of superfluid ^{4}He at low temperatures and under saturated vapor pressure[5]. The cartoon inset is a schematic picture of roton reproduced from Ref [6][p. 331].

The elementary excitation spectrum of He-II is shown in Figure 2. At small wavevectors ($Q \leq 0.7 \, \text{Å}^{-1}$), the elementary excitations are *phonons*, the quanta of pressure-density waves. The modes in the intermediate range around $Q \approx 1.1 \, \text{Å}^{-1}$ are referred to as *maxons*. The excitations near the local minimum of the spectrum are known as *rotons*. Close to this minimum, the excitation spectrum is approximately parabolic: $E_R(Q) = \Delta + \hbar^2(Q - Q_R)^2/2\mu$, where Δ is the roton energy gap, Q_R is the wavevector at the minimum, and μ is the effective mass of the roton. The nature of the roton is not yet fully understood, despite intense theoretical study over many years. According to Feynman and Cohen, rotons are the quantum-mechanical analog of perfect smoke rings shrunk to atomic dimensions[6]. That is, rotons consist of an atomic-sized core and slow, dipolar backflow around this core. The Feynman-Cohen picture is shown schematically in the inset of Figure 2.

In this summer school experiment, we will examine the collective excitations of superfluid ^{4}He. In particular, we will examine the properties of the roton (the energy gap Δ, wavevector Q_R, and effective mass μ) as a function of temperature T and pressure P. Our goal is to understand the connection between the structure of the liquid, as described by the static structure factor $S(Q)$, and the collective excitation spectrum $E_{ph-r}(Q)$.

2 Inelastic Neutron Scattering

In this section, we will briefly review the theoretical background for inelastic neutron scattering studies of liquid ^{4}He. The kinematics of neutron scattering are illustrated in Figure 3. The scattering of a neutron from a sample is governed strictly by the conservation of momentum and energy. Suppose that a scattered neutron has initial momentum $\hbar\mathbf{k}_i$ and energy $E_i = \hbar^2 k_i^2/2m$ and final momentum $\hbar\mathbf{k}_f$ and energy $E_f = \hbar^2 k_f^2/2m$. The neutron transfers a momentum $\hbar\mathbf{Q} = \hbar\mathbf{k}_i - \hbar\mathbf{k}_f$ and energy $E = E_i - E_f$ to the sample.

Solving the scattering triangle shown in Figure 3 yields the following relations:

$$Q^2 = k_i^2 + k_f^2 - 2k_i k_f \cos 2\theta \tag{1}$$

$$\frac{\hbar^2 Q^2}{2m} = E_i + E_f - 2\sqrt{E_i E_f} \cos 2\theta \tag{2}$$

> *Given these kinematic relationships, what is the shape of a detector 'trajectory' in $Q - E$ space? That is, what is the locus of points in $Q - E$ space which are 'seen' by an individual detector which is fixed at a scattering angle of 2θ? Compare a direct geometry instrument (fixed E_i) with an indirect geometry one (fixed E_f).* **Hint:** $E = E_i - E_f$.

In an inelastic neutron scattering experiment, one measures the double-differential scattering cross section $d^2\sigma/d\Omega dE_f$. This is the probability that an incident neutron is scattered by the sample into solid angle $d\Omega$ with a final energy between E_f and dE_f. In the first Born approximation, $d^2\sigma/d\Omega dE_f$ is proportional to the (coherent) dynamic structure factor $S(Q, E)$:

$$\frac{d^2\sigma}{d\Omega dE_f} = \frac{N\sigma_{coh}}{4\pi} \frac{k_f}{k_i} S_{coh}(Q, E) \tag{3}$$

Bulk liquid helium is homogeneous and isotropic. Therefore, we do not need to consider the vector quantity $\mathbf{Q}$ and may instead discuss only the scalar quantity Q.

> *Why is the incoherent scattering cross section σ_{inc} of our liquid helium sample equal to zero?* **Hint**: *there are two reasons.*
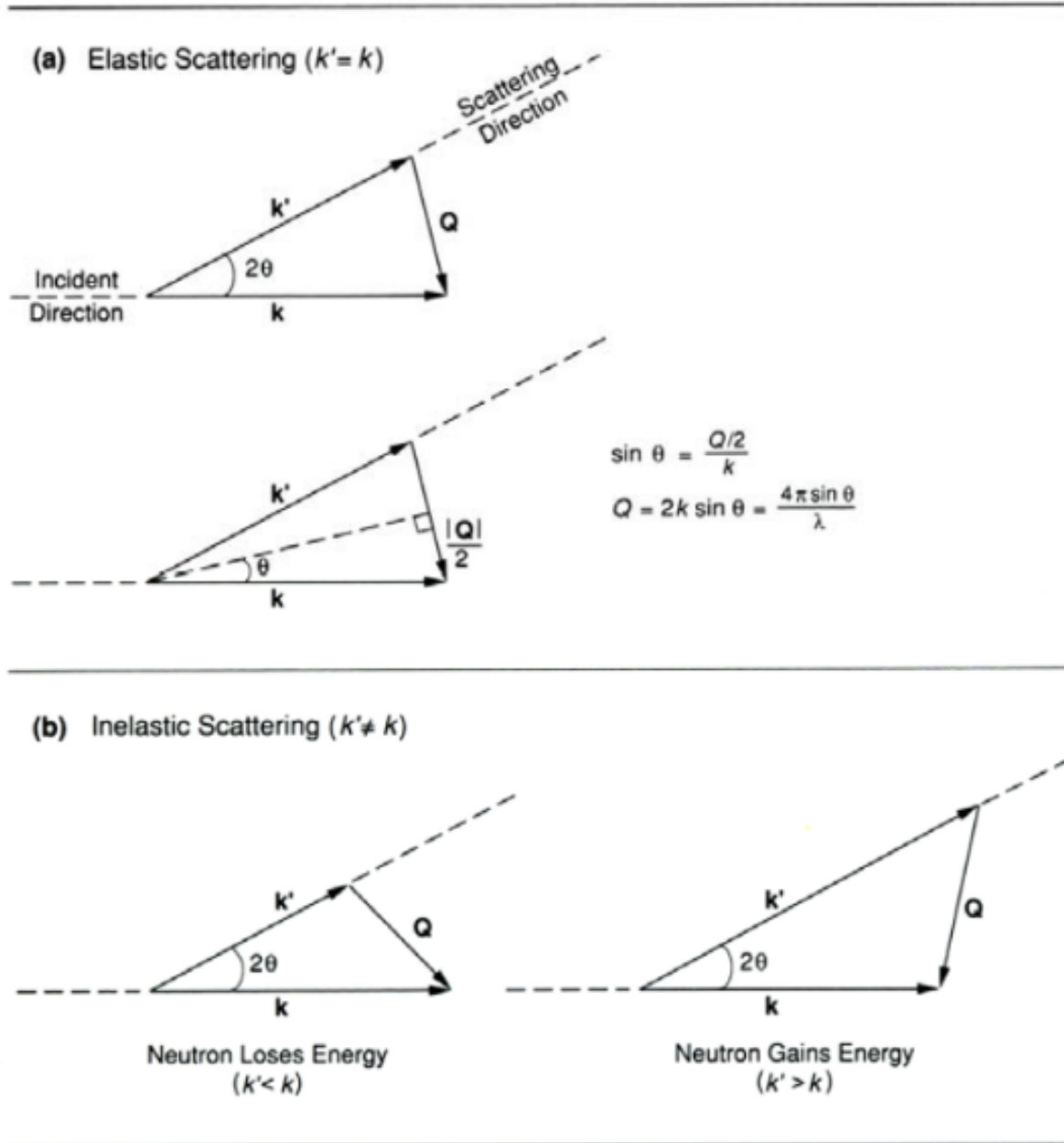
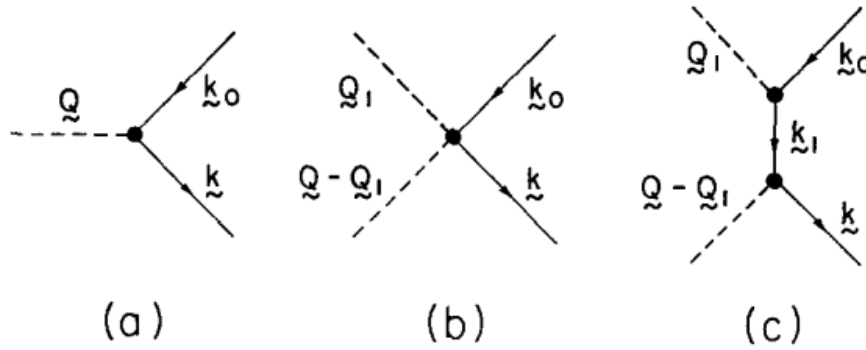Figure 3: The neutron scattering triangle as illustrated by Pynn[7].

Figure 4: Processes contributing to the measured signal in liquid helium[8]: (a) an incident neutron with wavevector $\mathbf{k}_0$ creates a *single* excitation of momentum $\hbar\mathbf{Q}$; (b) an incident neutron creates *two* excitations with combined momentum $\hbar\mathbf{Q}$; (c) an incident neutron undergoes *multiple scattering*, first creating an excitation with momentum $\hbar\mathbf{Q}_1$, then propagating to another point in the sample, and finally creating a second excitation with momentum $\hbar(\mathbf{Q} - \mathbf{Q}_1)$.

The dynamic structure factor $S(\mathbf{Q}, E)$ is the Fourier transform of the time-dependent, pair-correlation function $G(\mathbf{r}, t)$. In a classical liquid, $G(\mathbf{r}, t)$ is the relative probability that, given an atom located at $(0, 0)$, there is another atom at $(\mathbf{r}, t)$. In a quantum liquid, $G(\mathbf{r}, t)$ is the density-density correlation function.

Three different processes contribute to the observed scattering from He-II, and these are shown diagrammatically in Figure 4. First, an incident neutron may create a single phonon/maxon/roton excitation which carries away momentum $\hbar Q$ and energy E. Second, a neutron may undergo multiphonon scattering (i.e. create multiple excitations in a single scattering event). Finally, a neutron may undergo multiple scattering and create one or more excitations in each scattering event. It is only the first process which permits us to infer the dispersion relation from the observed scattering.

> *Can you explain why this is the case? What does single-phonon scattering contribute to $S(Q, E)$? What do you expect multiphonon scattering to contribute?*

An important relationship exists between neutron downscattering ($E > 0$) and neutron upscattering ($E < 0$) known as the *principle of detailed balance*. Suppose that the sample is in thermal equilibrium at temperature T. Then, $S(Q, E)$ obeys the following condition:

$$S(Q, -E) = e^{-E/k_B T} S(Q, E) \tag{4}$$

In general, the dynamic structure factor $S(Q, E)$ is asymmetric with respect to energy transfer E. The probability that a neutron will upscatter with energy transfer E is smaller than the probability that a neutron will downscatter with energy transfer E by a thermal factor $e^{-E/k_b T}$.

> *Suppose that your sample has an excitation with an energy of 1 meV. How large is the detailed balance effect at 2 K? 20 K? 200 K? How does this compare to a 1 μeV excitation? **Hint**: 1 meV = 11.6 K.*
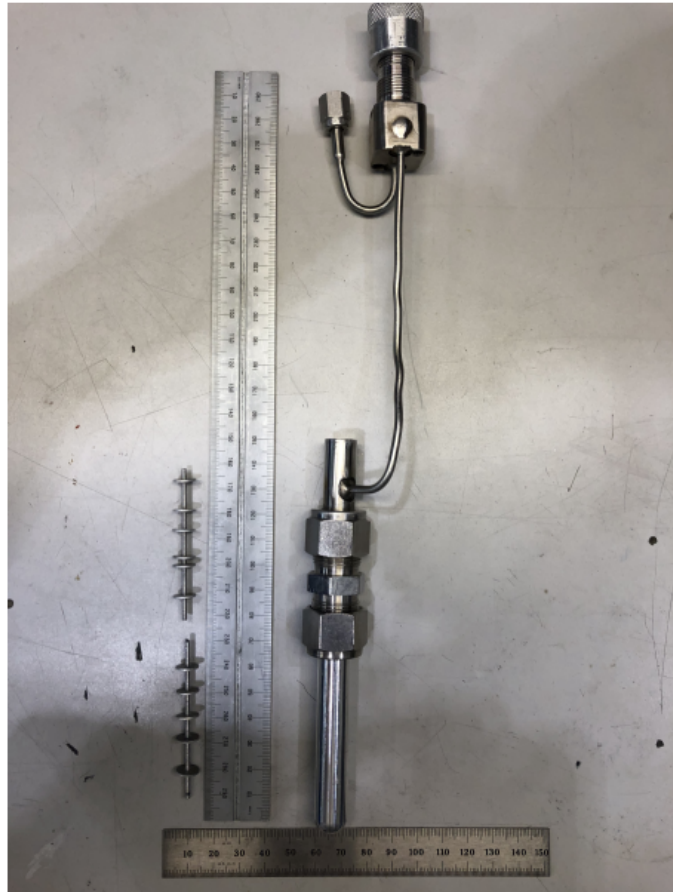
Figure 5: *Left:* An orange cryostat with a 70 mm bore. Technical details about orange cryostats and other sample environment setups are available on the NCNR Sample Environment website. *Right:* The pressure cell we will be using in this experiment.

3   Our Experiment

Here we briefly discuss our sample environment apparatus. Figure 5 displays a photograph of an *orange cryostat*, a type of continuous flow liquid helium cyrostat. These cryostats are used throughout the world at neutron sources, and they are sometimes referred to as "ILL cryostats" after the Institut Laue-Langevin. Orange cryostats are "top-loading" setups: the sample cell is connected to a stick, and this stick is inserted into the cryostat well from above. The well is filled with exchange gas that provides a thermal link between the sample cell and the cooling annulus of the cyrostat. The base temperature of an orange cryostat is typically around 1.5 K.

Helium gas is loaded to the sample cell *in situ* from an external gas handling system. We will use the cryostat to control the temperature of our sample and the gas handling system to control its pressure. The sample cell is shown on the right hand side of Figure 5. This particular pressure cell includes a cryogenic valve: no rubber o-rings, which are sure to fail at low temperature, are used. This setup is particularly useful whenever one wishes to dose gases to an (air-sensitive) sample, as is often done in experiments at NCNR. Load the sample material into the cell inside of a glove box; transport the cell to the stick while the cryogenic value is sealed; and finally open the cryogenic valve after the cell is attached to the gas fill line on the stick.

The dimensions of the sample are an important consideration in any neutron scattering experiment. The neutron scattering formalism turns on the assumption that a neutron interacts once with the sample. However, as illustrated in Figure 4, it is possible for a neutron to scatter multiple times before exiting the sample. There is no known *easy* way to correct the double-differential scattering cross section $d^2\sigma/d\Omega dE_f$ for the effects of multiple scattering. It is sometimes possible to approach multiple scattering corrections by using analytic models or by ray-tracing Monte Carlo simulations. Therefore, it is prudent to select a sample geometry so that the amount of multiple scattering is (hopefully!) negligible.

The effects of multiple scattering from liquid helium are discussed in detail in Ref [8]. These effects are expected to be small when the dimensions of the sample are much less than the mean-free path of the neutrons ($l = 1/\Sigma$). Liquid ^{4}He at a density of 0.145 g/cc possesses a macroscopic scattering cross section $\Sigma = 0.0293$ cm^{-1}. Our sample cell has a radius of $r = 0.5$ cm and a set of absorbing cadmium disks spaced every $d = 1$ cm. Thus, $\Sigma r = 0.0147$ and $\Sigma d = 0.0293$, which are both much less than one.

3.1   Sample Environment

3.2   How the Disk Chopper Spectrometer Works

We shall be performing this experiment using the Disk Chopper Spectrometer (DCS), a direct geometry (fixed incident energy E_i) time-of-flight spectrometer. In this type of instrument, pulses of monochromatic neutrons strike the sample at equally spaced times. The distance between the pulsing device to the sample D_{PS} and the distance from the sample to the detectors D_{SD} is known. Thus, the incident and final neutron energies, E_i and E_f, respectively, can be inferred from the time at which the pulse was created and the time at which the neutron was detected.

There are two methods of producing monochromatic pulses at a steady state neutron source, such as the cold source at NCNR. One method is to use a single crystal to monochromate the white beam and a mechanical chopper to pulse it; another technique is to use multiple choppers, such as the seven (!) choppers of DCS.

> *A monochromatic, pulsed beam of neutrons can be created using only two choppers. How does that work? Can you think of a reason why more than two choppers might be needed to make this a practicable method?*

The data acquisition system accumulates neutron counts (detection events) for each of the 913 DCS detectors. The time T between pulses is normally divided into 1000 channels of equal width, $\Delta t = 1000/T$.
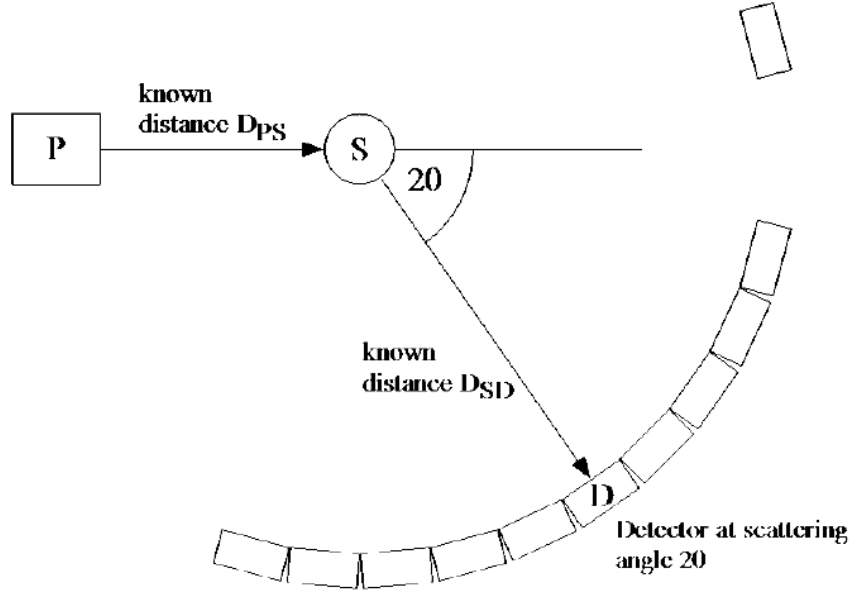
Figure 6: A schematic illustration of the scattering geometry of a direct geometry, time-of-flight spectrometer such as DCS.

Each detection event is registered in one of these channels. The data acquisition system generates a two-dimensional array of counts $N(i,j)$ as a function of detector index i and time channel j. This array is accumulated in a "histogramming memory" which is resident in the data acquisition computer. At the end of each run cycle, the array $N(i,j)$ is saved, along with other pertinent metadata, to the hard disk of the instrument computer.

In order to interpret the outcome of our experiment, we must transform the raw data $N(i,j)$ to the dynamic structure factor $S(Q,E)$. If we neglect self-shielding and multiple scattering effects, then the array $N(i,j)$ can be related to the double-differential scattering cross section:

$$N(i,j) = \frac{N_{BM}}{\eta_{BM}} \frac{d^2\sigma}{d\Omega dt_f} \Delta\Omega_i \Delta t N_m \eta_{ij} \tag{5}$$

Here $\Delta\Omega$ is the solid angle subtended by detector i; Δt is the width of the time channel; N_m is the number of sample molecules in the beam; η_{ij} is the efficiency of detector i for neutron detected in time channel j; N_{BM} and η_{BM} are the measured counts and efficiency, respectively, of the incident beam monitor.

We will not attempt to determine the dynamic structure factor $S(Q,E)$ in absolute units (1/meV) and will instead express it in terms of arbitrary units. This permits us to ignore all of the multiplicative factors in Equation 5 except for the detector efficiency function η_{ij}. To good approximation, the detectors of DCS are identical to one another. Thus, we can write $\eta_{ij} = \eta_{i0} f_j$, where η_{i0} is the efficiency of detector i for elastically scattered neutrons and a detector-independent function f_j that describes the energy-dependence of the detector efficiency. The correction for differences in detector response, i.e. the determination of η_{i0}, is performed using the results of a measurement with a vanadium sample.

The correction of the data for the energy dependence of the efficiency is achieved by calculation, knowing the various factors that affect the probability that a neutron is absorbed within a detector.

In order to obtain $d^2\sigma/d\Omega dE_f$ from $d^2\sigma/d\Omega dt_f$, we must change variables from time-of-flight to energy, including the Jacobian of the transformation. The energy of a neutron is related to its time-of-flight t over a fixed distance as $E \propto 1/t^2$. It follows that $dE \propto dt/t^3$. Hence, we may write:

$$\frac{d^2\sigma}{d\Omega dE_f} \propto \frac{d^2\sigma}{d\Omega dt_f}\left(\frac{dt}{dE_f}\right) \propto \frac{d^2\sigma}{d\Omega dt_f}t^3 \tag{6}$$

To obtain $S(Q,E)$, we either divide by k_f or, equivalently, multiply by another factor of t.

4 Analysis and Interpretation of the Scattering Data

4.1 Dispersion

We will begin our analysis by considering the $P = 0$ atm, $T = 1.5$ K data set. The dynamic structure factor $S(Q,E)$ of He-II at low temperatures can be expressed as sum of one-phonon scattering and multi-phonon scattering:

$$S(Q,E) = \underbrace{Z(Q)\delta(E - E_{ph-r}(Q))}_{\text{one-phonon}} + \underbrace{S_m(Q,E)}_{\text{multi-phonon}} \tag{7}$$

Here $E_{ph-r}(Q)$ is the dispersion of the phonon-roton spectrum; $Z(Q)$ is the integrated intensity of the one-phonon scattering; and $S_m(Q,E)$ is the multiphonon contribution.

4.2 Single Mode Approximation

The simplest theory that one can write down for the dynamic structure factor of He-II is the *single mode approximation*. According to this theory, only one-phonon processes significantly contribute to $S(Q,E)$. In other words, the contribution of multiphonon processes is negligible: $S_m(Q,E) \approx 0$.

$$S(Q,E) = Z(Q)\delta(E - E_S(Q)) \tag{8}$$

Starting from this assumption, we can predict both the dispersion relation $E_S(Q)$ and the integrated intensities $Z(Q)$. We appeal to the *sum rules* of coherent neutron scattering:

$$\text{zeroth moment sum rule:} \int_{-\infty}^{+\infty} S(Q,E)dE = S(Q) \tag{9}$$

$$f\text{-sum rule:} \int_{-\infty}^{+\infty} ES(Q,E)dE = \frac{\hbar^2 Q^2}{2M} \tag{10}$$

9

These sum rules are theorems of the neutron scattering formalism. The zeroth moment sum rule states that the integral of $S(Q, E)$ over all energies is equal to the *static structure factor $S(Q)$*. This function is the Fourier transform of the pair correlation function $g(r)$, which yields the relative probability of finding an atom a distance r from another one located at the origin. The f-sum rule states, in this case, that the first moment of the scattering is equal to the recoil energy of a helium atom, namely $\hbar^2 Q^2/2M$.

> *Use the sum rules to show that, in the single-mode approximation, $Z(Q) = S(Q)$ and $E_S(Q) = \hbar^2 Q^2/2MS(Q)$.*

> *Compare the predictions of the single mode approximation to your scattering data. Where does the theory work? And where does it break down? (For reference, $\hbar^2 = 4.18016$ meV amu Å^2 and $M = 4.00260$ amu.)*

4.3   Structure and Dynamics

Now that we have considered the $P = 0$ and $T = 1.5$ K data set, we turn to examining the phonon-roton spectrum at other thermodynamic conditions.

> *Use the zeroth moment sum rule to calculate the static structure factor $S(Q)$ of He-II at each pressure. What is the relationship between Q_R and the first peak in $S(Q)$?*

Dietrich *et al* argued that the number of atomic nearest neighbors is unchanged with temperature and pressure[10]. They obtained Q_R from inelastic neutron scattering measurements and found that it varies with the cube root of the liquid density, $Q_R = A\rho^{1/3}$. Different values of A correspond to different numbers of nearest neighbors: for simple cubic packing with six nearest neighbors, $A = 3.34$ cm $\text{g}^{-1/3}$ Å^{-1}; for bcc packing with eight nearest neighbors, $A = 3.65$ cm $\text{g}^{-1/3}$ Å^{-1}; and for hcp packing with twelve nearest neighbors, $A = 3.75$ cm $\text{g}^{-1/3}$ Å^{-1}.

> *Do your results agree with Dietrich et al? Do you find that the roton wavevector obeys $Q_R = A\rho^{1/3}$? If so, what value of A do you obtain?*

> *What quantity does a neutron diffractometer measure? Is it only elastic scattering? Hint: explain the relationship between $S(Q)$ and $S(Q, E = 0)$.*
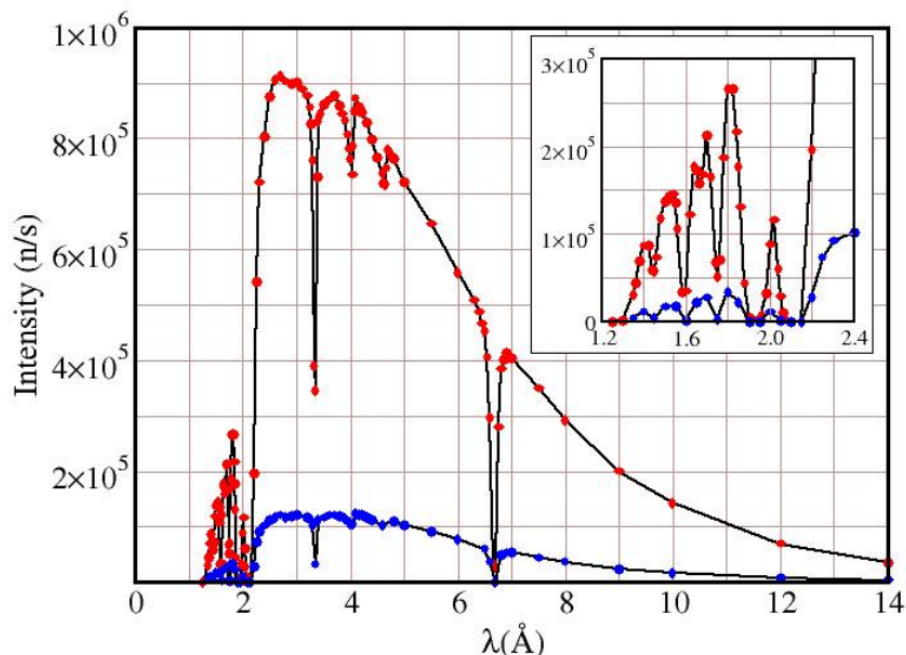
Figure 7: Incident flux as a function of neutorn wavelength λ. Red and blue points correspond to measurements using different chopper slot widths.

A Instrument Characteristics

The white beam from the cold neutron source is cleaned of high energy neutron and gamma ray contamination using an "optical filter". This is basically a bent guide which ensures that there is no line of sight from the source to points beyond the local shutter. A cooled graphite filter removes short wavelength (≈ 0.5 Å) neutrons that remain in the beam, permitting measurements at wavelengths down to roughly 1.5 Å.

A clean, pulsed, monochromatic neutron beam is produced using seven disk choppers. Chopper speeds may be varied from 1200 to 20000 rpm. The pulsing and monochromating choppers have three slots of different widths. In principle this permits three choices of intensity and resolution at a given wavelength and master chopper speed. The measured intensity at the sample is reproduced in Figure 7.

> *Why are there dips in the measured flux at wavelengths near* 3.335 *Å and* 6.67 *Å?*

The resolution of the instrument is approximately triangular and essentially independent of beam height (up to 10 cm) but depends slightly on the width of the beam. Hence samples should ideally be tall and thin rather than short and fat. The measured elastic energy resolution, for the same choices of chopper slot widths as in the intensity plot above, is shown in the Figure 8. Lines represent fits to the measurements.

An oscillating radial collimator, inside radius 200 mm, outside radius 300 mm, blade separation 2°, is used to reduce the scattering from sample environment structures.

> *Can you explain how the radial collimator works, and why it is oscillated?*

There are 913 six-atmosphere ^{3}He detectors covering an essentially continuous solid angle of ≈ 0.65 steradians and arranged in three banks:
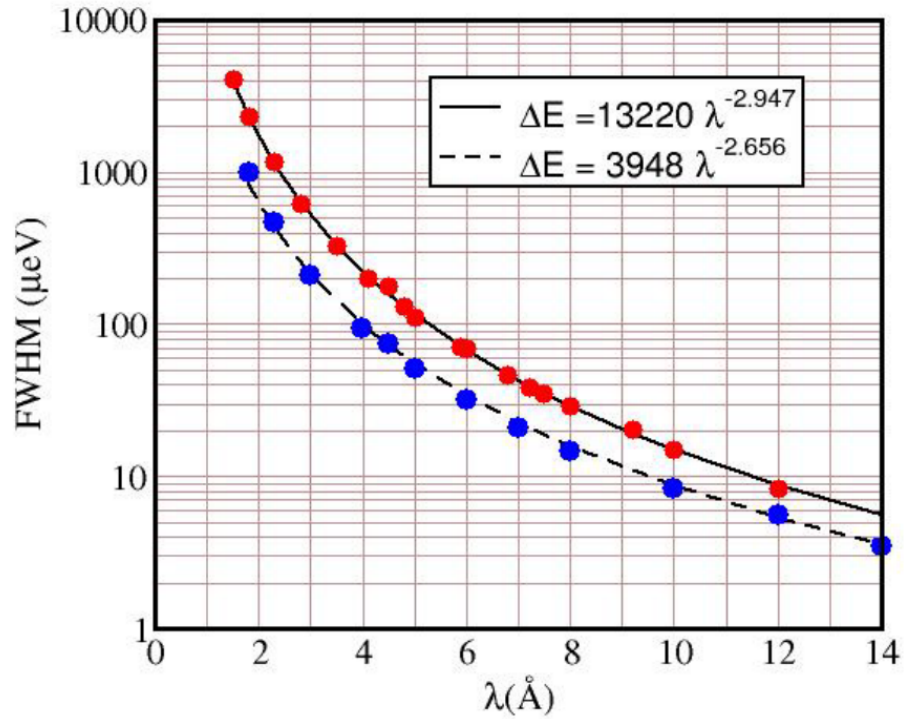
Figure 8: Elastic energy resolution of DCS as a function of incident wavelength λ.

- Middle bank detector scattering angles range from $-30°$ to $-5°$ and from $+5°$ to $+140°$

- Upper and lower bank angles range from $-30°$ to $-10°$ and from $+10°$ to $+140°$.

The flight distance from sample to detectors is 4010 mm. The flight chamber is purged with argon.

Why is the flight chamber purged with argon?

References

[1] J. M. Carpenter and C.-K. Loong, *Elements of Slow Neutron Scattering: Basics, Techniques, and Applications* (Cambridge University Press, 2015).

[2] A. Griffin, *Excitations in a Bose-Condensed Liquid* (Cambridge University Press, 1993).

[3] J. F. Annett, *Superconductivity, Superfluids, and Condensates* (Oxford University Press, 2004).

[4] L. Pitaevskii and S. Stringari, *Bose-Einstein Condensation and Superfluidity* (Oxford University Press, 2016)

[5] R. J. Donnelly and C. F. Barenghi, *J. Phys. Chem. Ref. Data* **27**, 1217 (1998).

[6] R. P. Feynman, *Statistical Mechanics: A Set of Lectures* (CRC Press, 1998).

[7] R. Pynn, "Neutron Scattering: A Primer" *Los Alamos Science* **19**, 1 (1990)

[8] V. F. Sears, "Slow-Neutron Multiple Scattering in Liquid Helium," *Nucl. Instrum. Methods Phys. Res* **123**, 521-527 (1975).

[9] J. S. Brooks and R. J. Donnelly, "The Calculated Thermodynamic Properties of Superfluid Helium-4" *J. Phys. Chem. Ref. Data*, **6**, 1 (1977).

[10] O. W. Dietrich, E. H. Graf, C. H. Huang, and L. Passell, "Neutron Scattering by Rotons in Liquid Helium" *Phys. Rev. B* **5**, 1377 (1972).